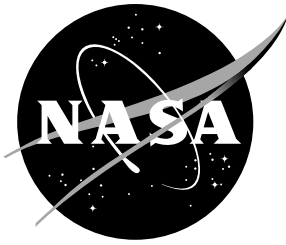


NASA Technical Memorandum 110309



# Evaluation of a Composite Sandwich Fuselage Side Panel With Damage and Subjected to Internal Pressure

Marshall Rouse and Damodar R. Ambur  
*Langley Research Center, Hampton, Virginia*

Jerry Bodine and Bernhard Dopker  
*Boeing Commercial Aircraft Company, Seattle, Washington*

February 1997

National Aeronautics and  
Space Administration  
Langley Research Center  
Hampton, Virginia 23681-0001

# **Evaluation of a Composite Sandwich Fuselage Side Panel With Damage and Subjected to Internal Pressure**

Marshall Rouse and Damodar R. Ambur  
NASA Langley Research Center  
Hampton, VA 23681-2331

Jerry Bodine and Bernhard Dopker  
Boeing Commercial Aircraft Company  
Seattle, WA

## **Abstract**

The results from an experimental and analytical study of a composite sandwich fuselage side panel for a transport aircraft are presented. The panel has two window cutouts and three frames, and has been evaluated with internal pressure loads that generate biaxial tension loading conditions. Design limit load and design ultimate load tests have been performed on the graphite-epoxy sandwich panel with the middle frame removed to demonstrate the suitability of this two-frame design for supporting the prescribed biaxial loading conditions with twice the initial frame spacing of 20 inches. The two-frame panel was damaged by cutting a notch that originates at the edge of a cutout and extends in the panel hoop direction through the window-belt area. This panel with a notch was tested in a combined-load condition to demonstrate the structural damage tolerance at the design limit load condition. The two panel configurations successfully satisfied all desired load requirements in the experimental part of the study, and the three-frame and two-frame panel responses are fully explained by the analysis results. The results of this study suggest that there is potential for using sandwich structural concepts with greater than the usual 20-in.-wide frame spacing to further reduce aircraft fuselage structural weight.

## **Introduction**

The potential for cost and weight reduction offered by composite-facesheet sandwich structures in aircraft fuselage side panels is currently being investigated in the NASA Advanced Composite Technology Program. Structural trade studies for sandwich concepts that use advanced material placement methods, such as tow placement for skin and three-dimensional braiding for frames, have identified a 25 percent cost and weight reduction compared to conventional integrally-stiffened metallic structures (Ref. 1). Sandwich structures offer additional potential for weight reduction by decreasing the number of frames by increasing the fuselage frame spacing. Sandwich structures are good candidates for implementing greater frame

spacing than the usual 20 to 22 in. frame spacing since skin panels for these structures have much higher bending stiffnesses than the more conventional stringer-frame stiffened skins with minimum gauge thicknesses. The sandwich panel described in the present paper has been designed to generate preliminary performance information for sandwich structures with twice the usual fuselage frame spacing.

The design studies for the curved panel described in the present paper utilized existing tension fracture data for flat sandwich panels which could result in conservative structural designs. Understanding the response of undamaged and damaged sandwich structures when they are subjected to combined loading conditions that are representative of the actual operating flight environment is an important aspect of designing aircraft structures. Very limited information currently exists for curved composite sandwich panels with damage at critical locations and subjected to combined loading conditions. To understand better the structural behavior of a sandwich fuselage side panel with windows and with damage at a highly stressed location, biaxial tension tests have been performed by subjecting the damaged panel to internal-pressure loading conditions.

Finite element analyses have been performed on the sandwich panel in the test machine and subjected to different test loading conditions. Inplane stress and strain results for an infinite composite flat plate with an elliptical cutout are compared with finite element analysis results to help explain the stress gradients along the cutout in the panel. The finite element analysis results are compared with experimental results for corresponding loading conditions. The present paper discusses the experimental results and their correlation with the analysis results.

### **Test panel and test description**

The sandwich fuselage panel considered in the present study has three frames and has overall dimensions of a 122-in. radius, a 72-in. length, and a 63-in. arc width. The panel has two window cutouts, one located midway between the center frame and each of the outer frames. The elliptical window cutouts are 19.92-in.-long in the fuselage circumferential direction and 15.30-in.-long in the fuselage longitudinal direction. The sandwich panel facesheets were fabricated from Hercules, Inc. AS4/8552 graphite-epoxy material and the core is made of a Hexcel Korex honeycomb material. The facesheet utilizes tow-placed inner plies and fabric outer layers. The fuselage frames and window frames were fabricated from fiber preforms consisting of triaxially braided AS4 graphite fibers impregnated with 3M Company PR500 epoxy resin and cured by using a Resin Transfer Molding (RTM) process. The sandwich skin and the precured frames are cocured in a single stage. Typical material properties for the tow placed, fabric, and triaxially braided AS4/8552 and AS4/PR500 graphite-epoxy material systems are presented in Table 1. Typical construction details of the test panel are shown in Figure 1. The cross-sectional view illustrates details of the panel in the window region. The sandwich core is contoured on both the concave and convex sides of the panel to accommodate  $\pm 45^\circ$  plies added to the 8-ply-thick

facesheet near the window region. When cured, the sandwich panel has a constant inner and outer mold line radius resulting in a uniform total thickness throughout the skin. Graphite-epoxy doublers fabricated from preimpregnated fabric were cocured with the curved and flat edges of the panel to introduce the axial and hoop loads into the panel skin. A photograph of the finished test panel is shown in Figure 2.

To evaluate the sandwich panel design, several tests were performed on the undamaged panel prior to inflicting damage in the form of a notch and re-evaluating the panel response using a pressure-box test machine described in Reference 1. In the undamaged condition, the panel was subjected to an axial load of 2,450 lb/in. with no internal pressure; a pressure only condition of 18.2 psi; and a combined load condition with 13.65 psi of internal pressure and 2,450 lb/in. of axial tension. The undamaged test conditions were also applied to the panel with its center frame removed to gather preliminary structural performance information on a panel with twice the initial frame spacing. A notch was then cut along the hoop direction starting at the window and extending through the window frame and the skin, and the panel was loaded to the design limit load condition of 8.85 psi of internal pressure and 1,630 lb/in. of axial tension. The panel was instrumented with electrical resistance strain gages to record strains and with displacement transducers to monitor panel displacements.

### **Finite element model**

The finite element model of the panel in the pressure-box test machine is shown in Figure 3. The sandwich panel is modeled using the ABAQUS finite element analysis program (Ref. 2) with 4-node isoparametric elements for the facesheets and three 8-node solid elements through-the-thickness to represent the honeycomb core. The ply drop-offs in the facesheets are discretely modeled to represent the thickness changes appropriately. The circumferential frames and the window frames are also modeled using the 4-node shell elements. The window glazing is also modeled using shell elements. Only reaction forces along the edges perpendicular to the window glazing are transmitted to the window frame. It is assumed that no inplane forces are transmitted to the panel.

The hoop and axial load introduction plates of the test fixture are modeled with shell elements. Since symmetry boundary conditions are assumed at the axial and hoop centerlines, only a quarter of the structure is modeled and analyzed. Along the sandwich panel hoop direction, the test fixture hoop-load-reaction turnbuckles for the skin and frames are represented with the appropriate length and stiffnesses to model the panel boundary conditions properly. Axial load is applied to the beams representing the hydraulic actuators attached to the axial load introduction plate. The quarter model of the test panel in the pressure box has a total of 5,343 elements and approximately 26,650 degrees of freedom. Geometric nonlinear analyses have been performed for all load cases considered in the present paper.

## Results and Discussion

The sandwich panel was modeled with the pressure-box test machine and was analyzed for critical loading conditions to determine the panel response both with and without damage. Some of the analytical results are compared with the experimental results in this section.

### Undamaged panel results

#### 2,450 lb/in. axial loading condition

The test panel was first analyzed for the 2,450 lb/in. ultimate loading condition for the axial loading condition. The inner and outer surface hoop strain contours obtained from the finite element analysis for this loading condition are presented in Figure 4. The influence of boundary conditions on the induced strain state in the panel can be seen in this figure. The abrupt variation in the strain state away from the edge of the elliptical cutout along its major axis is representative of the reduced hoop stiffness in the outer region of the panel. The maximum hoop strain corresponding to this loading condition is 1,580  $\mu\text{in./in.}$  and occurs on the panel inner surface at two locations along the edge of the window cutout at approximately 50° and 130° from the longitudinal axis of symmetry for the panel. The axial strain contours on the inner and outer surfaces of the panel are presented in Figure 5. A maximum axial strain of approximately 3,840  $\mu\text{in./in.}$  occurs at the 90° location along the window cutout on the panel outer surface. The analytically determined hoop and axial strain profiles around the elliptical cutout for an infinite flat plate made with the same ply stacking sequence are presented in Figure 6. These results are from a closed-form analysis method that utilizes a linear elastic solution and the method of superposition (Ref. 3) to determine the stresses and strains around the cutout. The hoop and axial strain results from this closed-form analysis are presented in Figure 6. These strain profiles compare very well with the panel outer surface strains along the window cutout obtained from the finite element analysis. The corresponding hoop and axial stress concentration factors, which are ratios of the stress magnitude at a given location along the cutout normalized by the far field stress, are plotted in Figure 6(b). The maximum value for the axial stress concentration factor is 3.57. The strain results from the test are presented in Figure 7(a) and 7(b). These strain values are measured at the locations along the edge of the window cutout indicated in Figure 7(c). The maximum experimental hoop and axial strains are 1,600  $\mu\text{in./in.}$  and 4,000  $\mu\text{in./in.}$ , respectively, and compare very well with the finite element analysis results. Local bending of the inner facesheet at the edge of the hole at the 90° location seems to have influenced the hoop and axial strain distribution as indicated in both the analytical and experimental results. For this reason, discussions of strain results for the other loading conditions are limited only to the panel outer facesheet.

### Combined 18.2 psi internal pressure and 1,110 lb/in. axial loading condition

This loading condition corresponds to twice the design limit pressure condition of 9 psi of internal pressure and a 1,110 lb/in. load in the panel axial direction. The outer surface hoop and axial strain variations along the elliptical hole edge obtained from the finite element analysis for this loading condition are presented in Figure 8. These results are compared with the analysis results presented in Figure 9 for a flat plate with an elliptical cutout. The hoop strain has a small negative value at the edge of the elliptical cutout near the major axis and the largest positive value along a radial line which is inclined at approximately 45° to the major axis. The axial strain results in Figure 9(a) indicate a large positive strain value at the edge of the elliptical cutout at the ellipse major axis and a small negative value at the boundary of the cutout at its minor axis. The finite element analysis results in Figure 8(b) are consistent with these results. The analytical stress concentration factor results presented in Figure 9(b) for an infinite flat plate suggest that the axial stress concentration factor is 3.01 for this loading condition.

The experimental strain results for this loading condition are presented in Figure 10. For the outer surface, the measured axial strain values at the minor axis is -1,000  $\mu\text{in./in.}$  and the value at the major axis is 2,200  $\mu\text{in./in.}$  The finite element analysis results at the corresponding locations are -662  $\mu\text{in./in.}$  and 1,420  $\mu\text{in./in.}$ , respectively.

### Combined 13.65 psi internal pressure and 2,450 lb/in. axial loading condition

This test condition corresponds to the design ultimate loading condition with 13.65 psi of internal pressure and 2,450 lb/in. of axial loading. The outer surface hoop and axial strain results from the finite element analysis are presented in Figure 11. The strain contours along the edge of the cutout agree well with the analytical results presented in Figure 12(a). These analytical results suggest that the hoop strain has a small negative value along the cutout boundary at the ellipse major axis and changes to a positive value at the ellipse minor axis. The axial strains are positive at the major axis and negative at the minor axis. The stress concentration factors from the infinite flat plate analysis are presented in Figure 12(b). For this loading condition, which has high tensile forces in both the panel axial and hoop directions, the stress concentration factors are 2.88 and 2.05 for the hoop and axial stresses, respectively, at the edge of the cutout. The hoop and axial strain distributions from the experiment are presented in Figure 13. The trends of the experimental results agree extremely well with the finite element analysis results. The experimentally measured strains on the panel outer surface in the hoop direction vary from 1,150  $\mu\text{in./in.}$  to -900  $\mu\text{in./in.}$  compared to the finite element analysis results which vary from 937  $\mu\text{in./in.}$  to -949  $\mu\text{in./in.}$  In the axial direction, the measured strains vary from 4,000  $\mu\text{in./in.}$  to -775  $\mu\text{in./in.}$  The corresponding results from the finite element analysis vary from 3,540  $\mu\text{in./in.}$  to -815  $\mu\text{in./in.}$

Neither of the above loading conditions resulted in strain magnitudes that exceed the strain allowables for the material systems used for manufacturing the test panel. There were no other indications from the experiment that suggested test panel failure. Further testing was conducted and it was assumed that the panel was in the pristine condition at the end of all the previous tests.

### **Results for the panel with the center frame removed**

The next set of loading conditions was imposed on the panel with the center frame removed. The objective of these tests was to gather preliminary information on the sandwich panel response with an increased frame spacing of 40.0 inches. The frame was removed by severing the frame web above the frame attachment flange at the skin. The finite element analysis and experimental results corresponding to two load conditions for this panel configuration are presented below.

#### Combined 18.2 psi internal pressure and 1,110 lb/in. axial loading condition

The finite element analysis results for this loading condition are presented in Figure 14. The hoop and axial surface strains are presented in the figure for the outer facesheet. The test was conducted by redistributing the loads in the severed frame to the remaining two frames to ensure that the panel is evaluated for the same load ratio of 80 and 20 percent of the load in the skin and the frames, respectively, for a given loading condition. The frame load for the panel with two-frame configuration is greater than that for the frame load for the panel with the three-frame configuration. This increase in frame load is indicated by comparing of results for the two-frame panel presented in Figure 14 with the results for the three-frame panel in Figure 4. The hoop strain in the remaining two frames increases by approximately 25 percent and the hoop strain in the skin between the two cutouts increases by approximately 12 percent due to the severing of the center frame. This increase in skin hoop strain is due to bending of the unsupported skin between the cutouts. The axial strain results from the finite element analysis for the inner facesheet are presented in Figure 15(a). Bending of the skin between the frames is also present for the inner and outer facesheet hoop strain contours. The experimental axial strain results for this panel are presented in Figure 15(b). The outer facesheet hoop strains from the experiment vary from approximately -400  $\mu\text{in./in.}$  to 2,200  $\mu\text{in./in.}$  compared to the finite element results which vary from -770  $\mu\text{in./in.}$  to 2,100  $\mu\text{in./in.}$  Bending of the skin between the two cutouts can be noticed in Figure 15(b) and is indicated by the differences in the experimental hoop strains for the inner and outer panel surfaces at  $\theta = 0$ . The axial strain results for this panel configuration corresponding to this loading condition are very similar to those for the panel with a three-frame configuration.

#### Combined 13.65 psi internal pressure and 2,450 lb/in. axial loading condition

The panel outer surface hoop and axial strain results from finite element analysis are presented in Figure 16 for this loading condition. The overall observations for the axial and hoop strains for this loading condition are very similar to

the previous loading condition for the two-frame panel. The experimental strain results for the two-frame panel are compared with the three-frame panel results in Figure 17. The maximum experimental axial strain along the cutout for the two-frame panel varies from  $-850 \mu \text{ in./in.}$  to  $4,000 \mu \text{ in./in.}$  compared to the analytical results which vary from  $-540 \mu \text{ in./in.}$  to  $3,860 \mu \text{ in./in.}$  These strain magnitudes are comparable to the axial strains for the three-frame panel for the same load condition. Bending of the skin between the frames is also observed for this loading condition and is similar to that observed for the previous loading condition for the two-frame panel.

The panel with the two-frame configuration responds in a predictable manner and the strain magnitudes for this loading condition are well within the strain allowables for failure initiation.

### **Results for the panel with a removed center frame and a notch at one cutout**

This test case is the final test case considered in the present study. A maximum value for the undamaged test panel axial strain occurs at the edge of the elliptical cutout at its major axis. The magnitude of the maximum strain is  $3,860 \mu \text{ in./in.}$  for the combined  $13.65 \text{ psi}$  internal pressure and  $2,450 \text{ lb/in.}$  axial loading condition. Damage in the form of a  $1\text{-in.}$ -long saw-cut notch was inflicted at this critical location to study the damage tolerance of this sandwich panel concept with a combined loading condition with  $8.85 \text{ psi}$  of internal pressure and  $1,630 \text{ lb/in.}$  of axial load. This loading condition corresponds to  $2/3$  of the design ultimate load condition. The notch was machined into the panel to extend in the panel hoop direction slightly beyond the window frame edge. The panel outer surface hoop and axial strain results from the finite element analysis are presented in Figure 18 for this combined loading condition. The hoop strain for this loading condition varies from  $-1,100 \mu \text{ in./in.}$  at  $\theta = 90^\circ$  to  $1,900 \mu \text{ in./in.}$  at  $\theta = 0^\circ$ . The strain magnitudes are significantly higher for this loading condition than for the hoop strain results presented in Figure 16 for the combined loading condition with  $13.65 \text{ psi}$  of internal pressure and  $2,450 \text{ lb/in.}$  of axial loading which are  $66$  percent lower. This increased strain state in the panel for this test case is due to the notch causing more panel bending in the skin between the two cutouts. The axial strain results from the finite element analysis for the outer surface indicate that a maximum strain of approximately  $5,200 \mu \text{ in./in.}$  occurs at the tip of the machined notch. The experimental strain results for this load case are presented in Figure 19. The axial strain results vary from  $-500 \mu \text{ in./in.}$  to  $5,800 \mu \text{ in./in.}$  and compare very well with the analysis results. No growth in the notch length was observed during the test.

The experimental hoop strain results along Line CC in Figure 1 for the three-frame panel, for the two-frame panel, and for the two-frame panel with a notch at the window cutout are compared in Figure 20. These results suggest that the far field strains in the hoop direction are influenced more by the removal of the frame than by the introduction of the notch. The increase in the panel strain state due to introducing the notch is local and does not result in any significant load redistribution.

## Concluding Remarks

The response of a sandwich fuselage side panel with two window cutouts has been evaluated for internal pressure and axial tension. The panel has been tested in a three-frame configuration with combined loading conditions that are representative of the design limit load and design ultimate load conditions. The strain magnitudes around the cutouts on the inner and outer surfaces of the test panel for these loading conditions are within the design ultimate strain allowable value of 4,000  $\mu$  in./in. for the material, suggesting that the structure satisfies the design requirements. The inner facesheet exhibits more local bending in the cutout region than does the outer facesheet. The strain states corresponding to the applied load conditions in an infinite composite flat plate were used to identify the differences in strain distributions between the inner and outer facesheets of the sandwich panel. The magnitude of the axial stress concentration factor is higher (3.57) for the axial loading condition, and the hoop stress concentration factor is higher (2.88) for the combined loading condition with 13.65 psi of internal pressure and 2,450 lb/in. of axial loading. Although the absolute values for the stress concentration factors determined from the flat plate analyses are not directly applicable to the curved panel studies in the present investigation, the locations for the maxima and the relative magnitudes of stress concentrations for different loading conditions are comparable. The finite element analysis results compare very well with the experimental results.

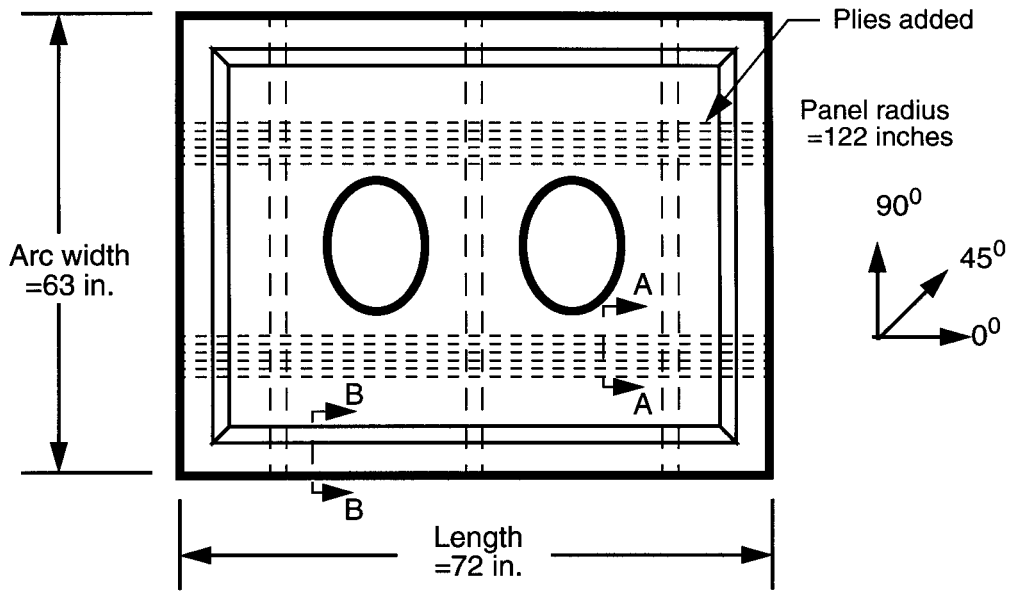
The finite element analysis results correlate very well with the experimental strain values for the panel with a two-frame configuration, and the strain results are less than the ultimate strain allowables for the material. The damage tolerance of the two-frame configuration is also demonstrated by testing the panel at design limit load conditions with a notch at a window cutout region that is in the location of the highest value of axial stress. For this case, the maximum value for the axial strain obtained from the test and from the analysis is approximately 5,200  $\mu$  in./in. with no growth in the notch length. This result suggests that the panel with twice the original frame spacing is capable of sustaining the design ultimate load conditions without damage and of sustaining the design limit load conditions with a 1-in.-long notch. This finding from the experiments is significant considering that reducing the number of frames results in a lighter weight structure.

## References

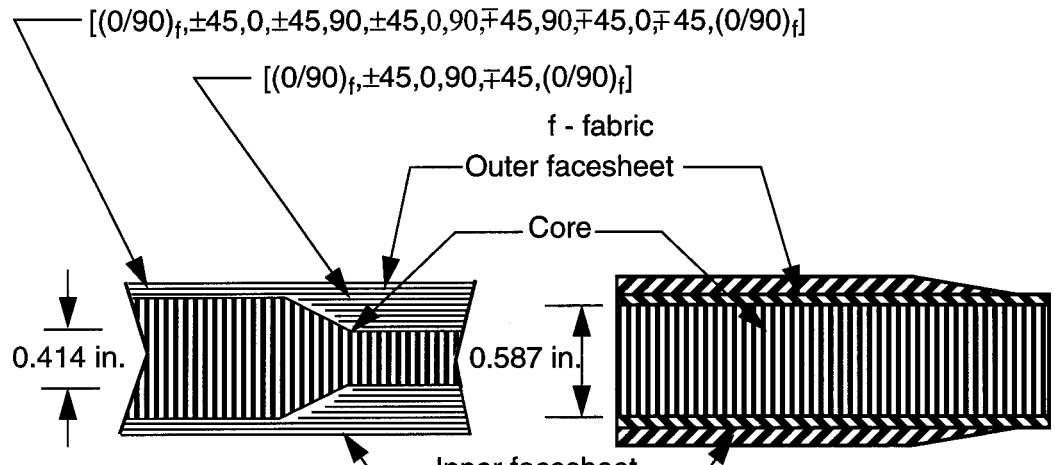
1. Rouse, M.; and Ambur, D. R.: Evaluation of Damaged and Undamaged Fuselage Panel Responses Subjected to Internal Pressure and Axial Load. Sixth NASA/DoD/ARPA ACT Conference, Anaheim, CA, August 7-11, 1995.
2. Anon.: ABAQUS Finite Element Code. Hibbitt, Carlson and Sorenson, Inc., Vol. 1-2, 1995.
3. Savin, G. N.: Stress Concentrations Around Holes. Pergamon Press, London, 1961.

Table 1. Typical material properties for the graphite-epoxy materials used to manufacture the sandwich panel.

Property	Tow AS4/8552	Fabric AS4/8552	Triaxial braid AS4/PR500	Korex core
Longitudinal modulus, $E_1$ (Msi)	18.30	9.20	7.50	0.00001
Transverse modulus, $E_2$ (Msi)	1.36	9.20	7.50	0.00001
Lateral modulus, $E_3$ (Msi)	1.36	1.30	----	0.0340
In-plane shear modulus, $G_{12}$ (Msi)	0.76	0.72	0.57	0.00001
Transverse shear modulus, $G_{23}$ (Msi)	0.52	0.50	0.40	0.0136
Transverse shear modulus, $G_{13}$ (Msi)	0.76	0.50	0.57	0.0326
Major Poisson's ratio, $\nu_{12}$	0.32	0.04	0.29	0.30



a. Plan view of the panel.



b. Cross-sectional view "AA"

c. Cross-sectional view "BB"

Figure 1. Construction details for the sandwich panel.

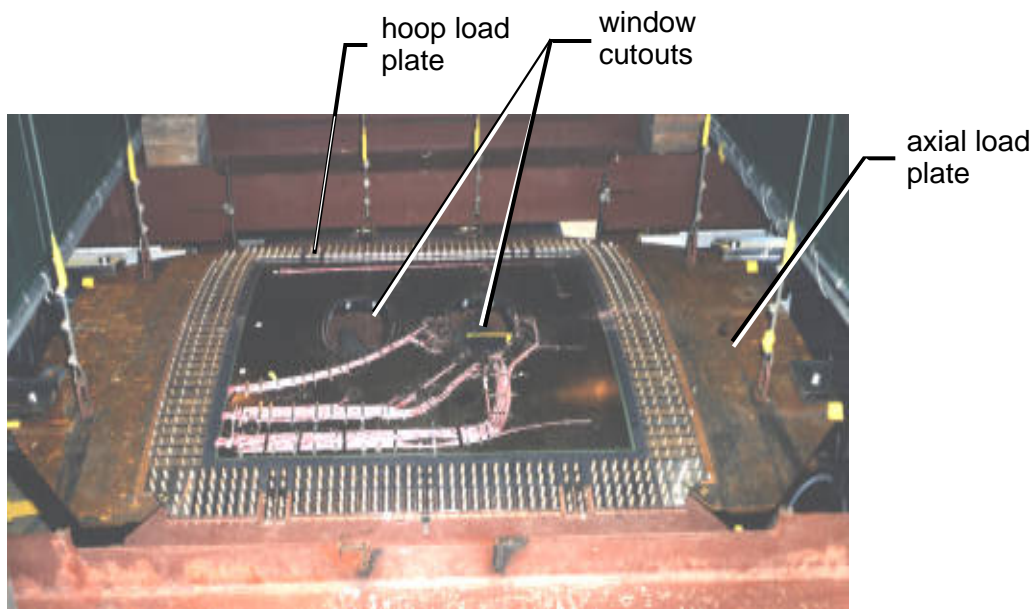


Figure 2. Photograph of the sandwich panel.

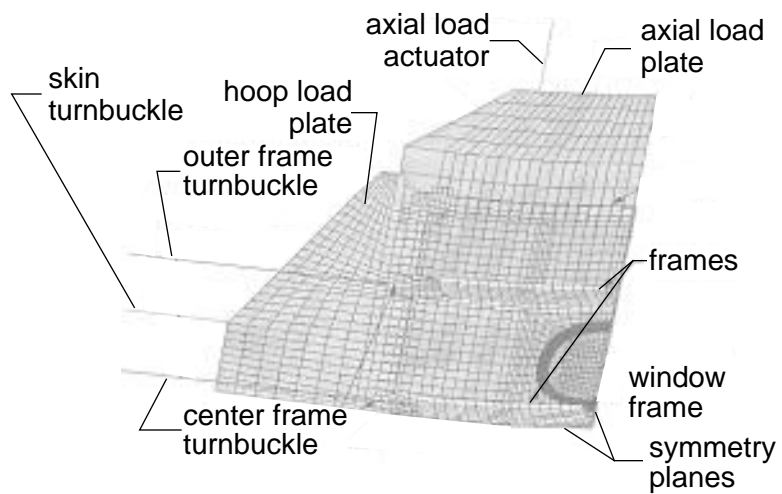


Figure 3. Finite element model of the sandwich panel.

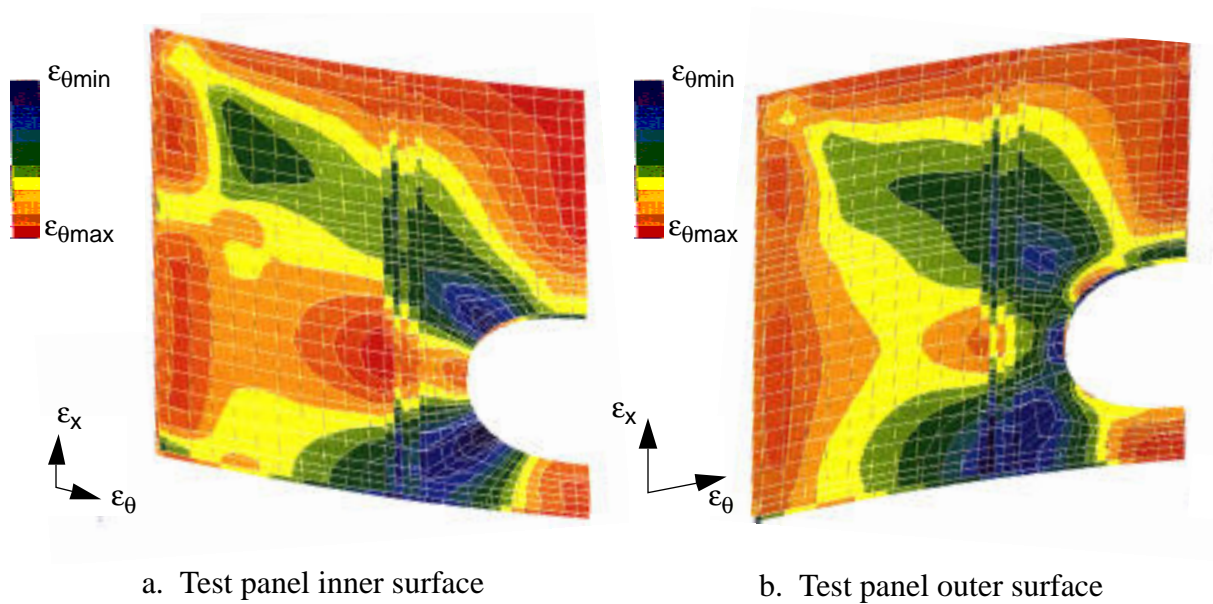


Figure 4. Hoop strain from the finite element analysis results for 2,450 lb/in. axial loading condition.

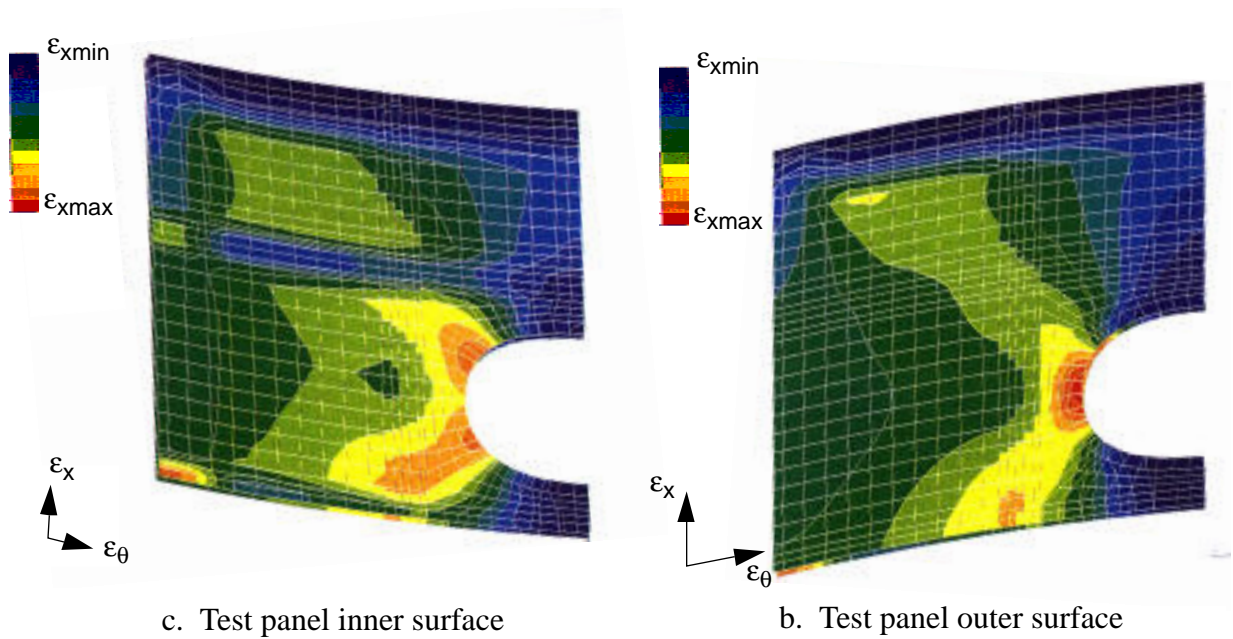


Figure 5. Axial strain results from the finite element analysis for the 2,450 lb/in. axial loading condition.

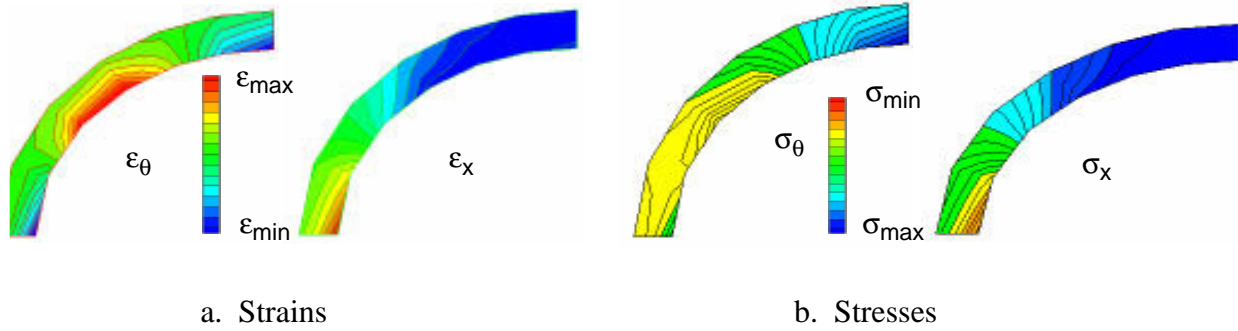


Figure 6. Analytical results for a flat plate with an elliptical hole and subjected to 2,450 lb/in. of axial load.

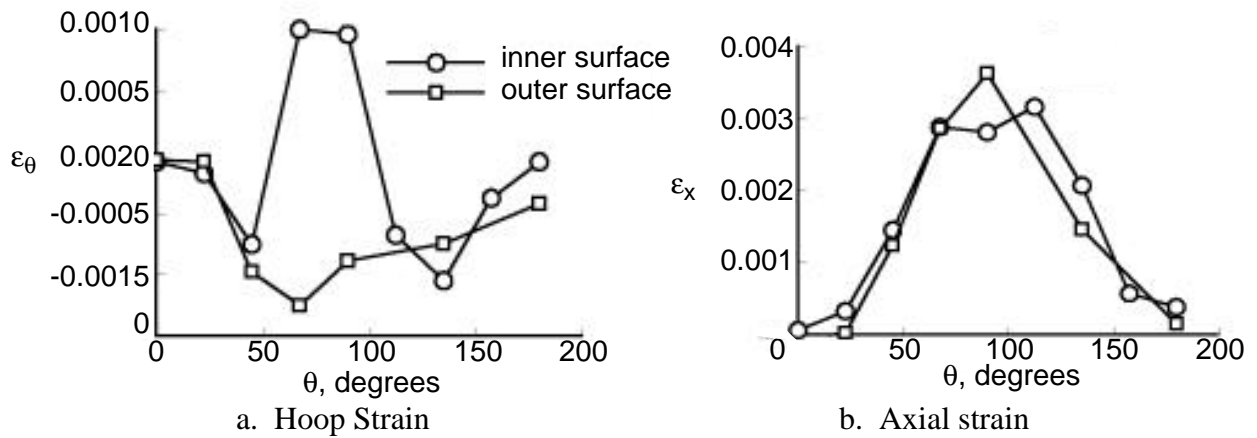


Figure 7. Experimental strain results for the 2,450 lb/in. axial load condition.

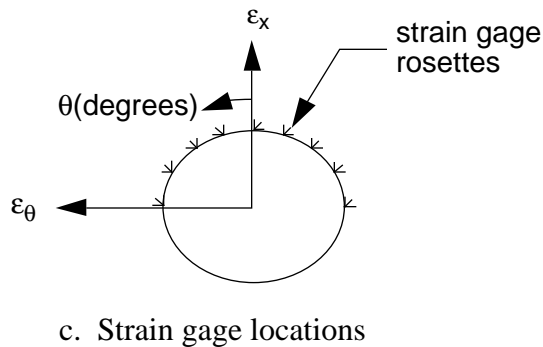


Figure 7. Concluded.

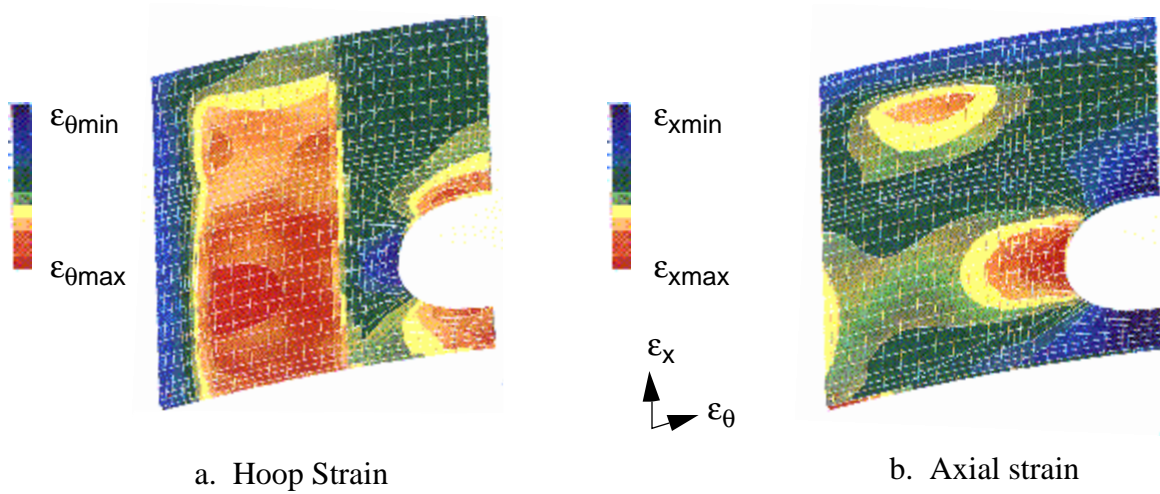


Figure 8. Finite element analysis results for strains on the panel outer surface for a combined 18.2 psi internal pressure and 1,110 lb/in. axial loading condition.

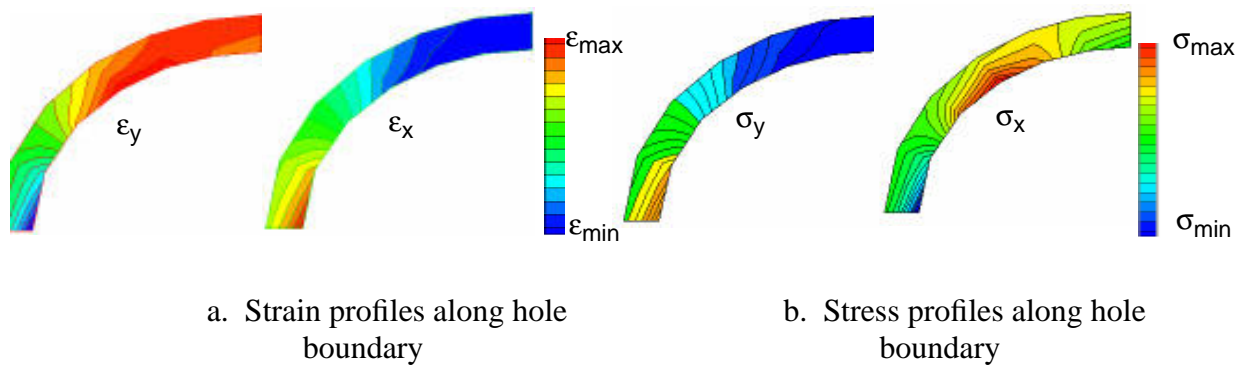
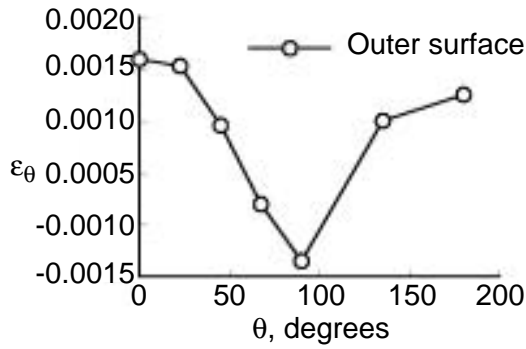
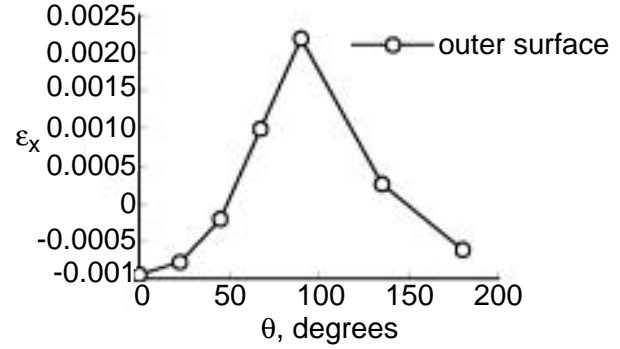


Figure 9. Analytical results for a flat plate with an elliptical hole and subjected to combined 18.2 psi internal pressure and 1,110 lb/in. axial loading condition.

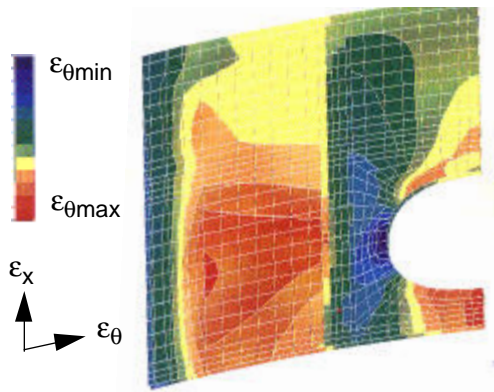


a. Hoop strain

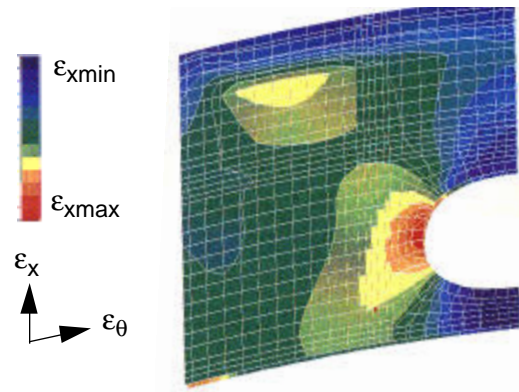


b. Axial strain

Figure 10. Experimental strain results for a combined 18.2 psi and 1,110 lb/in. axial loading condition.

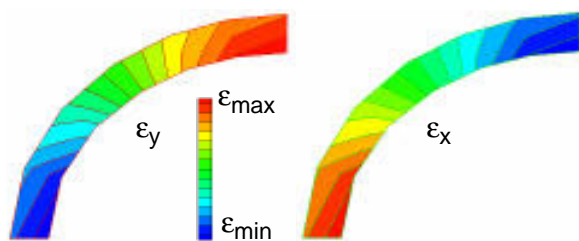


a. Hoop strain

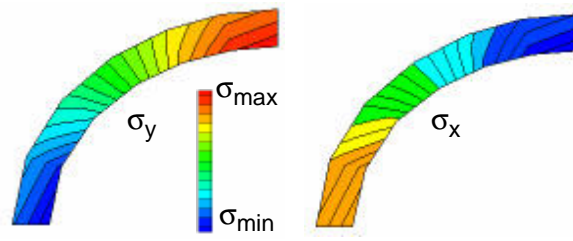


b. Axial strain

Figure 11. Finite element analysis results for strain contours on the panel outer surface for a combined 13.65 psi internal pressure and 2,450 lb/in. axial loading condition.

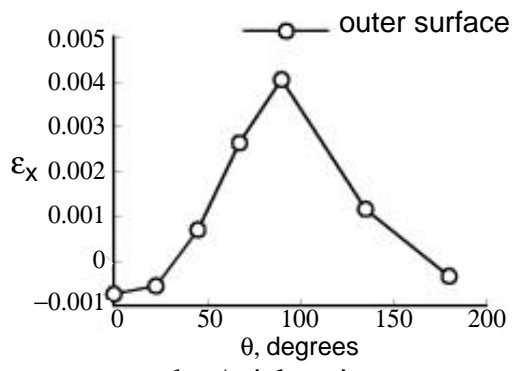
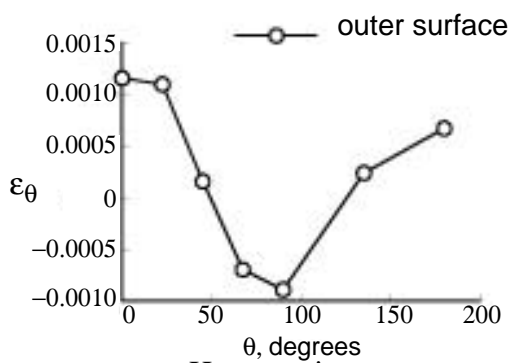


a. Strain profiles along the hole boundary



a. Stress profiles along the hole boundary

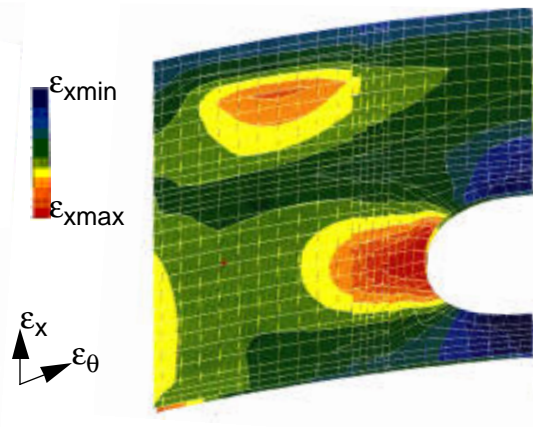
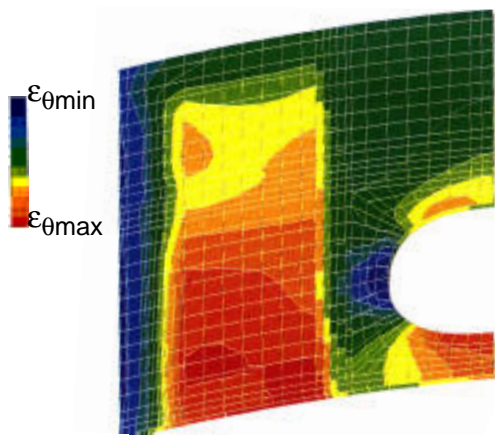
Figure 12. Analytical results for a flat plate with an elliptical hole and subjected to a combined 13.65 psi internal pressure and 2,450 lb/in. axial loading condition.



a. Hoop strain

b. Axial strain

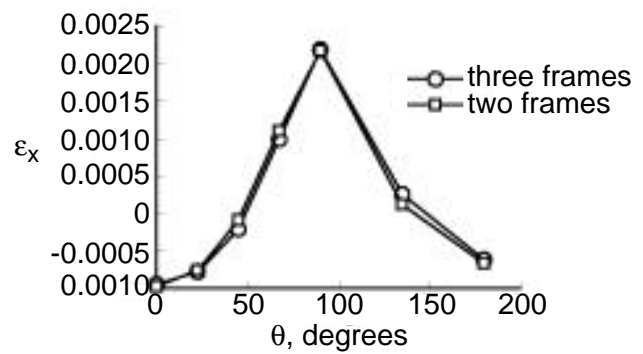
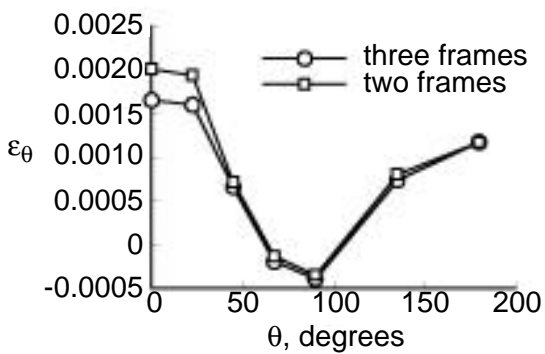
Figure 13. Experimental strain results for a combined 13.65 and 2,450 lb/in. axial loading condition.



a. Hoop strain

b. Axial strain

Figure 14. Finite element analysis results for strains on the two-frame panel outer surface for a combined 18.2 psi internal pressure and 1,110 lb/in. axial loading condition.



a. Hoop strain

b. Axial strain

Figure 15. Experimental strain results on the two-frame panel outer surface for a combined 18.2 psi and 1,110 lb/in. axial loading condition.

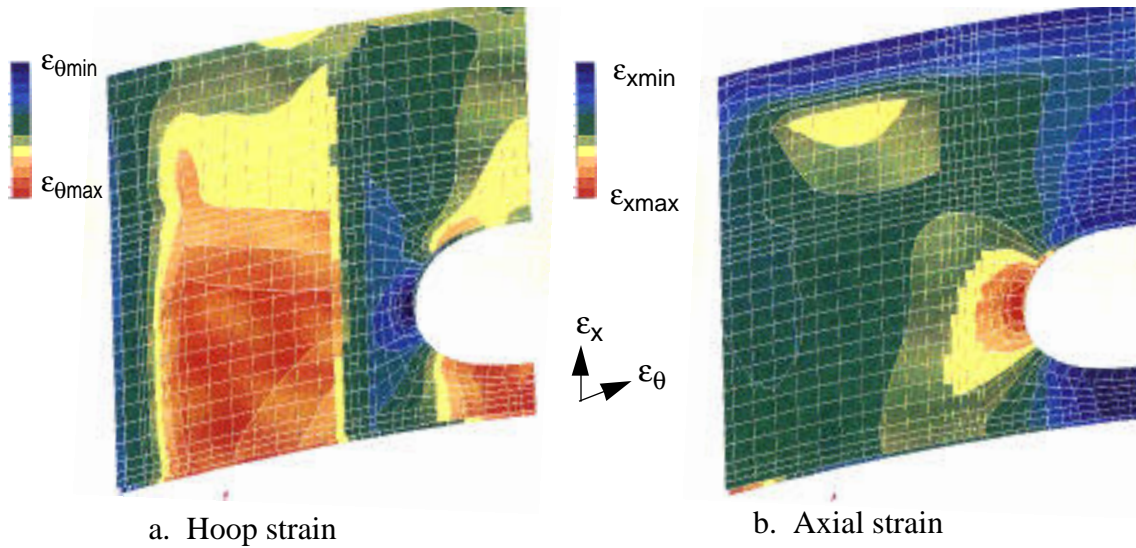


Figure 16. Finite element analysis results for strains on the two-frame panel outer surface for a combined 13.65 psi internal pressure and 2,450 lb/in. axial loading condition.

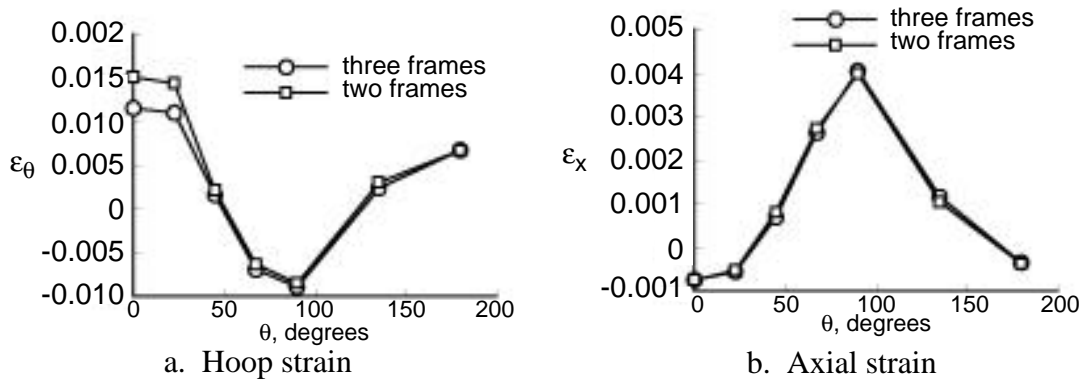


Figure 17. Experimental strain results on the two-frame panel outer surface for a combined 13.65 psi internal pressure and 2,450 lb/in. axial loading condition.

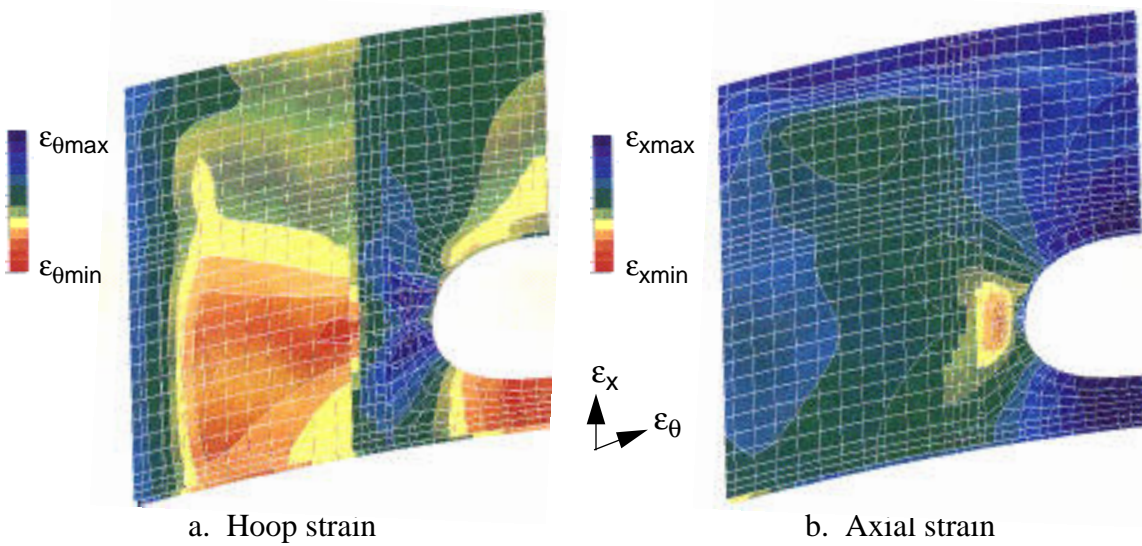


Figure 18. Finite element analysis results for strains on the notched two-frame panel outer surface for a combined 8.85 psi internal pressure and 1,630 lb/in. axial loading condition.

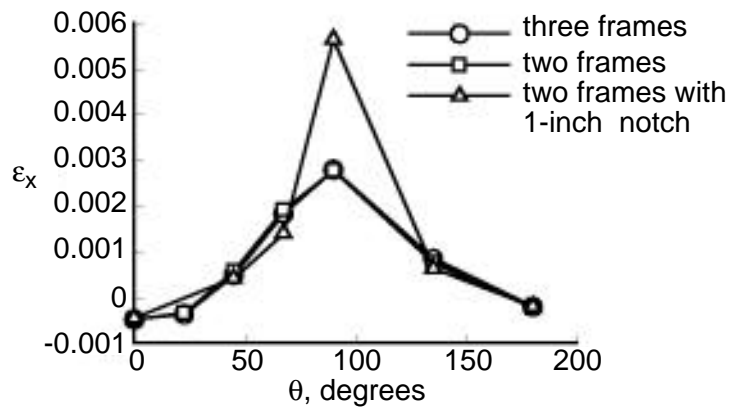


Figure 19. Experimental axial strain results on the notched two-frame panel outer surface for a combined 8.85 internal pressure and 1,630 lb/in. axial loading condition.

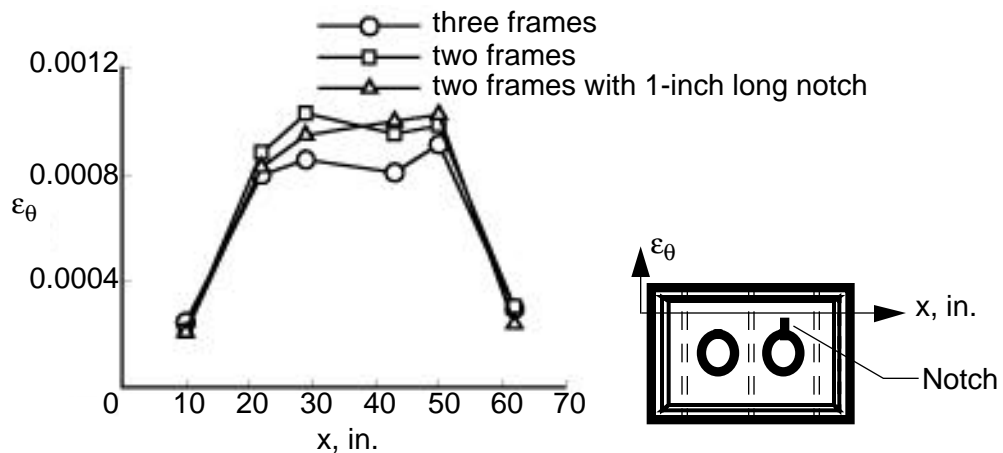


Figure 20. Comparison of experimental far-field outer service hoop strain results for the three-frame, two-frame, and notched two-frame panels.